Published in final edited form as:
Minim Invasive Ther Allied Technol. 2013 September ; 22(5): . doi:10.3109/13645706.2013.788028.

Image quality improvements in C-Arm CT (CACT) for liver oncology applications: Preliminary study in rabbits

Vania Tacher[1], **Nikhil Bhagat**[1], **Pramod P. Rao**[1], **MingDe Lin**[2], **Dirk Schäfer**[3], **Niels Noordhoek**[4], **Peter Eshuis**[4], **Alessandro Radaelli**[4], **Eleni Liapi**[1], **Michael Grass**[3], and **Jean-François Geschwind**[1]

[1]Johns Hopkins Hospital, Interventional Radiology, Baltimore, MD, USA [2]Philips Research North America, Briarcliff Manor, NY, USA [3]Philips Research, Hamburg, Germany [4]Philips Healtcare, Best, The Netherlands

Abstract

Introduction—C-Arm CT (CACT) is a new imaging modality in liver oncology therapy that allows for the acquisition of 3D images intra-procedurally. CACT has been used to enhance intra-arterial therapies for the liver by improving lesion detection, avoiding non-target embolization, and allowing for more selective delivery of agents. However, one of the limitations of this technology is image artifacts created by respiratory motion.

Purpose—To determine in this preliminary study improvements in image acquisition, motion compensation, and high resolution 3D reconstruction that can improve CACT image quality (IQ).

Material and methods—Three adult male New Zealand white rabbits were used for this study. First, a control rabbit was used to select the best x-ray acquisition imaging protocol and then two rabbits were implanted with liver tumor to further develop 3D image reconstruction and motion compensation algorithms.

Results—The best IQ was obtained using the low 80 kVp protocol with motion compensated reconstruction with high resolution and fast acquisition speed (60 fps, 5 s/scan, and 312 images).

Conclusion—IQ improved by: (1) decreasing acquisition time, (2) applying motion-compensated reconstruction, and (3) high resolution 3D reconstruction. The findings of this study can be applied to future animal studies and eventually could be translated into the clinical environment.

Keywords

C-arm CT; interventional oncology; intra-arterial therapy; TACE

Introduction

C-Arm CT (CACT) is a technique in which an angiographic unit equipped with a flat panel detector is used to obtain CT-like images. These images are able to eliminate any vessel superposition that is seen in digital subtraction angiography (DSA) and provide improved

Correspondence: V. Tacher, Johns Hopkins Hospital, Russel H. Morgan Department of Radiology and Radiological Science, Division of Interventional Radiology, 1800 Orleans Street, Baltimore MD 21287, USA, vaniatacher@gmail.com.

Declaration of interest: The other authors have no relevant financial disclosure.

soft tissue contrast. CACT has many potential applications (1,2), including improving neurointerventional (3), oncological (4), and cardiac procedures (5).

Recently, CACT has been used for interventional oncology procedures, especially during intra-arterial therapies in the liver (6). There are numerous improvements that CACT provides over projection based imaging such as DSA and fluoroscopy, including better lesion detection, more selective delivery of agents, and avoidance of non-target embolization (4,7–10). More recently, a dual phase CACT acquisition during the early arterial and delayed parenchyma phase has been proposed to characterize tumors (and to potentially determine treatment success) before and after therapy (11,12).

Although this technology is extremely promising in the interventional oncology arena, improvement and optimization of the imaging process with respect to data acquisition, image reconstruction and post-processing is a task of current medical imaging research. In our current clinical protocol, each phase of the dual phase scan takes ten seconds to acquire, which requires the patient to be at end-expiration apnea. Image degradation due to respiratory motion limits CACT's ability to detect, target, and assess tumor response of hepatocellular carcinoma for transarterial chemoembolization treatment (11,13). In our experience, more than half of the transarterial chemoembolization (TACE) patient cases experienced significant motion artifact that limited CACT's utility. Although there has already been research in the arena of image quality and breathing motion compensated reconstruction (14–16), there are currently no commercially available motion compensation tools for CACT.

The purpose of this study was to improve CACT IQ by improved image acquisition, specifically by increasing scan speed and incorporating image reconstruction with motion compensation and increased resolution (17). These improvements were developed and tested in combination with image reconstruction at different resolution levels on a clinical C-arm system that is used only for animal studies. The advantage of using a clinical system for animal studies is two-fold:

- we can apply findings to future animal studies, and
- eventually translate these findings into the clinical environment.

Material and methods

All animal studies were approved by our institution's Animal Care and Use Committee (ACUC). All procedures were conducted under their guidelines.

Animals

Three adult male New Zealand white rabbits weighing between 3.8–4.3 kgs (Myrtle's Rabbitry, Thompson Station, TN, USA) were used for this preclinical study. First, a tumor-less control rabbit (C) was used to select the best x-ray acquisition imaging protocol. Then, two other rabbits (R1 and R2) were implanted with VX2 liver tumor, as described in previous work (18), to develop 3D image reconstruction and motion compensation algorithms. These animals were also subjects of a study evaluating performance of drug-eluting bead embolization in a VX2 rabbit model, for which an imaging protocol needed to be established. The current study describes a secondary objective of that study, to formulate a standardized, reliable, and effective CACT image acquisition protocol.

Anesthesia

For treatment, the animals were pre-medicated with an intramuscular injection of acepromazine (2.5 mg/kg; Phoenix, St. Joseph, MO, USA) and ketamine hydrochloride

(Ketaject, 44 mg/kg; Phoenix, Clipper Distributing Company, Llc, St. Joseph, MO, USA). Sedation was maintained with propofol (10 mg/ml, APP Pharmaceuticals, Schaumburg, IL, USA) in monitored boluses of 2 mg (0.25 ml) intravenously via the right marginal ear vein. The rabbits were free breathing at 30–60 breaths/min. Post procedure, analgesic buprenorphine (0.02–0.05 mg/kg) was injected intramuscularly for pain relief. Euthanasia was achieved by injecting a bolus of ketamine hydrochloride. The control animal was anesthetized once as described above (same as that of R1 and R2 during treatment).

Trans-arterial chemo-embolization (TACE) procedure

For R1 and R2, an incision was made in the skin and subcutaneous structures after shaving, disinfecting, and draping the right inner thigh and groin. Blunt dissection was performed to expose the right femoral artery. A 3 French introducer (Check-Flo, Cook, Bloomington, IN, USA) was introduced over a guide wire through the femoral arterial access. Next, the hepatic artery was catheterized using a 2 French JB1 catheter (Cook Bloomington, IN, USA) over a 0.014” guide wire (Transcend, Boston Scientific, Miami, FL, USA). TACE was performed using 100–300 microns diameter drug-eluting beads (LC Beads, Biocompatibles, Oxford, CT, USA) loaded with Doxorubicin (DEB-TACE).

Imaging and post processing

All animal imaging was performed using a commercial C-arm system (Allura FD20 with XperCT option, Philips Healthcare, Best, the Netherlands). Contrast medium (Oxilan 300 mg I/ml, Guerbet LLC, Bloomington, IN, USA) diluted in a 1:5 ratio with saline (1.5 ml total injected volume) was manually injected during CACT. Image quality (IQ) evaluation was based on visual assessment of image contrast, presence of artifacts, characterization of landmarks (abdominal aorta, ribs, and vertebra), and tumor delineation (for R1 and R2). The assessments were performed by three interventional radiologists. The CACT image acquisition and post processing methodology was as follows:

- the x-ray acquisition technique that provided the best IQ using available commercial protocols and a prototype protocol was found on the control rabbit (Figure 1)
- R1 and R2 were imaged using the results from above and then different image reconstruction methods were applied. These include image reconstruction with and without motion compensation using different image matrix sizes with a voxel size adapted ramp filter.

CACT was acquired in the control animal using 120 kVp at 200 and 150 mA with variations of scan time and frames per second (fps) (Table I) using commercially available protocols. A low voltage prototype protocol (P4) of 80 kVp, 85 mA, 5 ms with 60 fps and 5-second scan time (sc) was also used to acquire CACT images based on prior work in small animals (19). The total angular range covered in a 10 (5) sec acquisition was 208° (205°) for each rotational run. Two protocols (P3, P4) produced the best IQ and were then used to image the tumor-bearing rabbits (R1 and R2) in order to compare the different image reconstruction methods.

R1 was imaged using P3 (120 kVp, 150 mA, 5 ms, 60 fps), and R2 was imaged using P4 (80 kVp, 85 mA, 5ms, 60 fps). R1 was sacrificed after DEB-TACE and served as a control for IQ comparison (the post mortem rabbit had no motion). CACT was acquired immediately post TACE *in-vivo* for the tumor bearing rabbits (R1 and R2) and additionally after sacrifice in R1. The images were then post processed using:

- standard 3D reconstruction,

- standard 3D reconstruction + prototype motion compensation, and
- high resolution 3D reconstruction + prototype motion compensation.

Standard 3D reconstruction used a 256 × 256 × 192 matrix with 0.98 mm^3 voxel size. High resolution 3D reconstruction used a 512 × 512 × 384 matrix with 0.49 mm^3 voxel size. The standard and high resolution reconstructions were computed using the commercially available filtered back projection algorithm on the imaging system. To achieve reconstructions at different resolution levels, a band limited ramp filter with voxel size adapted maximum frequency was used within the filtered back projection reconstruction. The prototype motion compensation algorithm (MC) aligned the projection images by calculating the shift of the diaphragm visible in the projections. The motion vector field is interpolated from the diaphragm motion while assuming fixed bone position in the 3D volume during the rotational run. This motion vector field is used within the reconstruction algorithm to correct the ray geometry according to the motion vector field (16,17,20,21). Since it is also based on cone beam filtered back projection, reconstruction at different resolution levels is realized as above.

Results

Image acquisition protocol selection

Initial assessment of image quality (IQ) for x-ray acquisition protocol selection was based on image contrast, presence of image artifacts, and characterization of landmarks including the abdominal aorta, ribs, and vertebra. The control rabbit (C) was imaged with commercially available protocols and a prototype protocol (Figure 1a,1b,1c,1d). Of the three commercially available protocols (1a–c), the 120 kVp, 150mA, 5 ms, 60 fps protocol P3 (Figure 1c) showed the best IQ. The liver parenchyma IQ seemed equivocal with the other protocols but the bone outlines were better defined. The prototype x-ray technique (Figure 1d) showed the best IQ of all protocols tested in this study. The fat planes were better seen with the interface between the planes and the muscles or other soft tissues. Similarly, the liver margins and boundaries were better seen compared to the other acquisition protocols. Also better seen were the aorta, paravertebral muscles, and the bony structures such as the ribs and the vertebral bodies. There was overall better IQ with the low kVp protocol. It should also be noted that the two best protocols used 5-second scan times. Though a lower number of projection images were acquired compared to protocol P2, the faster scan had a shorter time window and so was less affected by ventilation motion. In general it should be mentioned that the ventilation pattern has small variations from scan to scan resulting in different artifact strength and distribution.

3D reconstruction and motion compensation

Based on the results above on x-ray technique selection, Rabbit 1 (R1) was imaged using the best commercially available protocol and Rabbit 2 (R2) was imaged using the prototype protocol. R1 and R2 had implanted VX-2 liver tumors. The acquired images were processed using reconstruction with standard resolution, motion compensated reconstruction with standard resolution, and motion compensated reconstruction with high resolution (Figure 2).

The subsections below describe the results in more detail.

- Reconstruction with standard resolution

  R2 (Figure 2b) images using standard reconstruction was better than R1 (Figure 2a). Standard reconstruction images of R2 revealed a better tumor delineation (arrows) than those of R1, however a point of argument could be that the size of the tumor was smaller in R1. Tumor contrast fixation was well visualized on R2 but the

margins and outlines were not as well characterized. Similarly intra-tumoral contrast fixation and hypodensities (areas with poor contrast uptake) were poorly characterized. R1 images with standard reconstruction revealed an ill-defined hypodense area in the left lobe of the liver, which could be assumed to be a tumor, however the image quality was not sufficient to characterize the lesion.

- Motion compensated reconstruction with standard resolution

  With application of motion compensated reconstruction (17,19,20) to the standard reconstructions (Figure 2c and 2d) there was a slight improvement in the IQ when compared to standard reconstruction alone. The presence of tumor in R1 (Figure 2c) could be better appreciated with the addition of motion compensation; however, tumor characterization was still a challenge. R2 (Figure 2d) images were marginally better than without motion compensation.

- Motion compensated reconstruction with high resolution

  There was overall more noise in the high resolution reconstructed images, making them grainier, but there was considerable improvement in IQ. Tumor margins were better visualized in R1 (Figure 2e) than the previous steps of post-processing improvement. However no further tumor characterization was possible (limitation of the x-ray acquisition). The liver margins, bones, and muscles were very well visualized compared to the standard reconstruction with or without motion compensation. Tumor characterization in R2 (Figure 2f) was very good, with sharper tumor margins (arrows). The contrast fixation in the tumor post-TACE was very well seen and the fixation pattern could be better appreciated. Areas of strong contrast fixation post-TACE (representing viable treated areas of tumor) could be differentiated from areas of moderate (representing a zone between vascularized and non-vascular areas) and poor fixation (non-vascularized, hypodense areas-necrotic areas). Similarly with regards to normal anatomy, the bones (vertebrae and ribs) were very well characterized and their margins and marrow areas were well defined. The aorta and the muscles with their respective fat planes were better defined. An example includes a small lumbar artery seen in the left para-aortic region.

  To compare the IQ between ideal conditions of complete apnea and motion compensated images, CACT was performed post harvest of R1 (Figure 2g) and the images processed using standard reconstruction. Among the combinations of post-processing for R1 when imaged alive, the high resolution reconstruction with the prototype motion compensation showed IQ that most closely resembled the post-mortem scan.

Discussion

The main finding of this preliminary study was that a combination of improved imaging protocol, motion compensation, and high resolution 3D reconstruction improved CACT image quality in an animal model. Some of these findings could translate into the clinical environment. Details of the study findings are below.

Improved imaging protocol – the scan time was decreased from ten seconds to five seconds by doubling the gantry speed. Though fewer x-ray projection images were acquired compared to protocol P2 and a higher detector binning was used, which all resulted in lower spatial resolution, the faster scan reduced the temporal window for breathing motion artifacts and showed improved IQ. It is expected that this finding can be translated to the clinical environment, but it needs to be proven. Furthermore, the low kVp x-ray technique

showed improved IQ compared to the standard 120 kVp technique. This is due to the improved x-ray contrast at lower photon energies (19,22). For the standard 32 cm computed tomography dose index (CTDI) phantom improved contrast to noise ratio (CNR) for iodine contrast studies has been shown with the low kVp protocol used in this study (23). In the clinical situation, a compromise between the physical size of the scanned patient and the applied mean spectrum energy needs to be chosen, especially for patients with large body mass index.

Motion compensation – CACT allows for the acquisition of a three dimensional data set from the use of a flat panel detector during the interventional procedure. The 3D dataset, as compared to fluoroscopy, has improved tissue contrast and spatial resolution. These advantages are important in interventional oncology, especially intra-arterial liver directed therapies. This is primarily because there is superposition of many vessels in a small volume. CACT has been shown to improve sensitivity of tumor detection (11,12) and make the intra-arterial therapy more effective and safe as compared to fluoroscopy alone (4,7–10). However, a major limitation to this technology is image degradation caused by motion artifacts such as ventilation. A recent study showed that acquiring two phases of CACT (dual phase), one depicting the early arterial phase and the other depicting the delayed parenchyma phase, is more sensitive in detecting tumors than one phase alone (24). Other studies have shown that dual phase CACT can detect the majority of lesions shown on contrast enhanced MRI of the liver and may help in distinguishing pseudolesions from HCC (11,12). Dual phase CACT is especially sensitive to motion artifacts, as both scans are compared and often times co-registered. In our experience, an assessment of 66 TACE patient cases between October 1, 2011-January 12, 2012, 41 cases (62%), experienced significant motion artifact that limited CACT's utility. Findings from this study on the improvement of IQ by use of motion compensation could be adapted for use in the clinical environment and potentially increase the sensitivity of CACT in detecting lesions.

High resolution reconstruction with motion compensation – a higher spatial resolution 3D reconstruction was used and then motion compensation applied. The high resolution kernel provided for increased spatial resolution, and resulted in sharper/more defined images. The IQ improved substantially. However, the motion compensation with the high resolution reconstruction requires more computer processing time (~ 5– 6 fold) as compared to standard reconstruction without motion compensation. In the pre-clinical environment this is not an issue because immediate image access as compared to the clinical environment usually is not required.

A limitation in this study is that because it was a secondary experiment, the availability of rabbits for a more systematic evaluation of the various protocols could not be done. Further work with more rabbits in a more step-wise fashion would be helpful to better confirm our findings. In addition, the small number of rabbits made quantitative assessment (and statistical comparisons) of IQ impossible; rather we relied on qualitative assessment of IQ for comparisons. Nevertheless, some findings such as increased acquisition speed can be more immediately/directly applied in the clinical environment while other findings such as motion compensation will require further testing and development. The findings of this study could help in improving clinical CACT IQ.

Acknowledgments

M. Lin, D. Schäfer, N. Noordhoek, P. Eshuis, A. Radaelli, and M. Grass are Philips employees. J.F. Geschwind is a consultant to Biocompatibles, Bayer Healthcare, Guerbet, Nordion, Merit, Abbott, and Jennerex. This study was funded by NIH/NCI R01 CA160771, P30 CA006973, Philips Research North America, Briarcliff Manor, NY, USA and the French Society of Radiology (SFR).

References

1. Wallace MJ, Kuo MD, Glaiberman C, Binkert CA, Orth RC, Soulez G. Three-dimensional C-arm cone-beam CT: applications in the interventional suite. J Vasc Interv Radiol. 2008; 19:799–813. [PubMed: 18503893]
2. Grass, M.; Guillemaud, R.; Rasche, V. Interventional X-ray Volume Tomography. In: Grangeat, P., editor. Tomography. London, UK: ISTE; 2010. p. 287-306.
3. Soderman M, Babic D, Holmin S, Andersson T. Brain imaging with a flat detector C-arm: Technique and clinical interest of XperCT. Neuroradiology. 2008; 50:863–868. [PubMed: 18560818]
4. Wallace MJ. C-arm computed tomography for guiding hepatic vascular interventions. Tech Vasc Interv Radiol. 2007; 10:79–86. [PubMed: 17980322]
5. Schwartz JG, Neubauer AM, Fagan TE, Noordhoek NJ, Grass M, Carroll JD. Potential role of three-dimensional rotational angiography and C-arm CT for valvular repair and implantation. Int J Cardiovasc Imaging. 2011; 27:1205–1222. [PubMed: 21394614]
6. Lin M, Loffroy R, Noordhoek N, Taguchi K, Radaelli A, Blijd J, et al. Evaluating tumors in transcatheter arterial chemoembolization (TACE) using dual-phase cone-beam CT. Minimally invasive therapy & allied technologies: Minim Invas Ther and Allied Technol. 2011; 20:276–281.
7. Tognolini A, Louie JD, Hwang GL, Hofmann LV, Sze DY, Kothary N. Utility of C-arm CT in patients with hepatocellular carcinoma undergoing transhepatic arterial chemoembolization. J Vasc Interv Radiol. 2010; 21:339–347. [PubMed: 20133156]
8. Wallace MJ, Murthy R, Kamat PP, Moore T, Rao SH, Ensor J, et al. Impact of C-arm CT on hepatic arterial interventions for hepatic malignancies. J Vasc Interv Radiol. 2007; 18:1500–1507. [PubMed: 18057284]
9. Hirota S, Nakao N, Yamamoto S, Kobayashi K, Maeda H, Ishikura R, et al. Cone-beam CT with flat-panel-detector digital angiography system: early experience in abdominal interventional procedures. Cardiovasc Intervent Radiol. 2006; 29:1034–1038. [PubMed: 16988877]
10. Sze DY, Razavi MK, So SK, Jeffrey RB Jr. Impact of multi-detector CT hepatic arteriography on the planning of chemoembolization treatment of hepatocellular carcinoma. AJR Am J Roentgenol. 2001; 177:1339–1345. [PubMed: 11717079]
11. Loffroy R, Lin M, Rao P, Bhagat N, Noordhoek N, Radaelli A, et al. Comparing the detectability of hepatocellular carcinoma by C-arm dual-phase cone-beam computed tomography during hepatic arteriography with conventional contrast-enhanced magnetic resonance imaging. Cardiovasc Intervent Radiol. 2012; 35:97–104. [PubMed: 21328023]
12. Miyayama S, Yamashiro M, Okuda M, Yoshie Y, Nakashima Y, Ikeno H, et al. Detection of corona enhancement of hypervascular hepatocellular carcinoma by C-arm dual-phase cone-beam CT during hepatic arteriography. Cardiovasc Intervent Radiol. 2011; 34:81–86. [PubMed: 20333382]
13. Loffroy R, Lin M, Yenokyan G, Rao P, Bhagat N, Noordhoek N, et al. Intra-Procedural C-Arm Dual-Phase Cone Beam CT Imaging to predict Response to Drug-Eluting Beads Transcatheter Arterial Chemoembolization in Patients with Hepatocellular Carcinoma ? Radiology. 2013; 266:636–648. [PubMed: 23143027]
14. Zhang Q, Hu YC, Liu F, Goodman K, Rosenzweig KE, Mageras GS. Correction of motion artifacts in cone-beam CT using a patient-specific respiratory motion model. Med Phys. 2010; 37:2901–2909. [PubMed: 20632601]
15. Rit S, Wolthaus JW, van Herk M, Sonke JJ. On-the-fly motion-compensated cone-beam CT using an a priori model of the respiratory motion. Med Phys. 2009; 36:2283–2296. [PubMed: 19610317]
16. Rao P, Lin M, Bhagat N, Schäfer D, Loffroy R, Pellerin O. Improving C-arm Cone Beam CT: Protocol Optimization and Reducing Motion Artifacts for Preclinical Imaging. RSNA. 2011:E353.
17. Schäfer D, Borgert J, Rasche V, Grass M. Motion-compensated and gated cone beam filtered back-projection for 3-D rotational X-ray angiography. IEEE Trans Med Imaging. 2006; 25:898–906. [PubMed: 16827490]

18. Lee KH, Liapi E, Buijs M, Vossen JA, Prieto-Ventura V, Syed LH, et al. Percutaneous US-guided implantation of Vx-2 carcinoma into rabbit liver: a comparison with open surgical method. J Surg Res. 2009; 155:94–99. [PubMed: 19181344]

19. Lin M, Samei E, Badea CT, Yoshizumi TT, Johnson GA. Optimized Radiographic Spectra for Small Animal Digital Subtraction Angiography. Med Phys. 2006; 33:4249–4257. [PubMed: 17153403]

20. Schäfer D, Lin M, Rao PP, Loffroy R, Liapi E, Noordhoek N, et al. Breathing motion compensated reconstruction for C-arm cone beam CT imaging: initial experience based on animal data. Medical Imaging 2012: Physics of Medical Imaging. 2012 83131D-D.

21. Lin, M.; Rao, P.; Loffroy, R.; Liapi, E.; Noordhoek, N.; Eshuis, P., et al. RSNA. Lakeside Learning Center; 2011. Improved C-Arm Cone-Beam CT Imaging in the Rabbit VX-2 Liver Tumor Model by Faster Image Acquisition and Compensating for Breathing Motion: First Results.

22. Kalender WA, Deak P, Kellermeier M, van Straten M, Vollmar SV. Application- and patient size-dependent optimization of x-ray spectra for CT. Med Phys. 2009; 36:993–1007. [PubMed: 19378760]

23. Schäfer D, Ahrens M, Eshuis P, Grass M. Low kV rotational 3D x-ray imaging for improved CNR of iodine contrast agent. Medical Imaging 2012: Physics of Medical Imaging: SPIE (International Society for Optical Engineering). 2011 83132V-V.

24. Meyer BC, Frericks BB, Voges M, Borchert M, Martus P, Justiz J, et al. Visualization of hypervascular liver lesions During TACE: comparison of angiographic C-arm CT and MDCT. AJR. 2008; 190:W263–W269. [PubMed: 18356419]

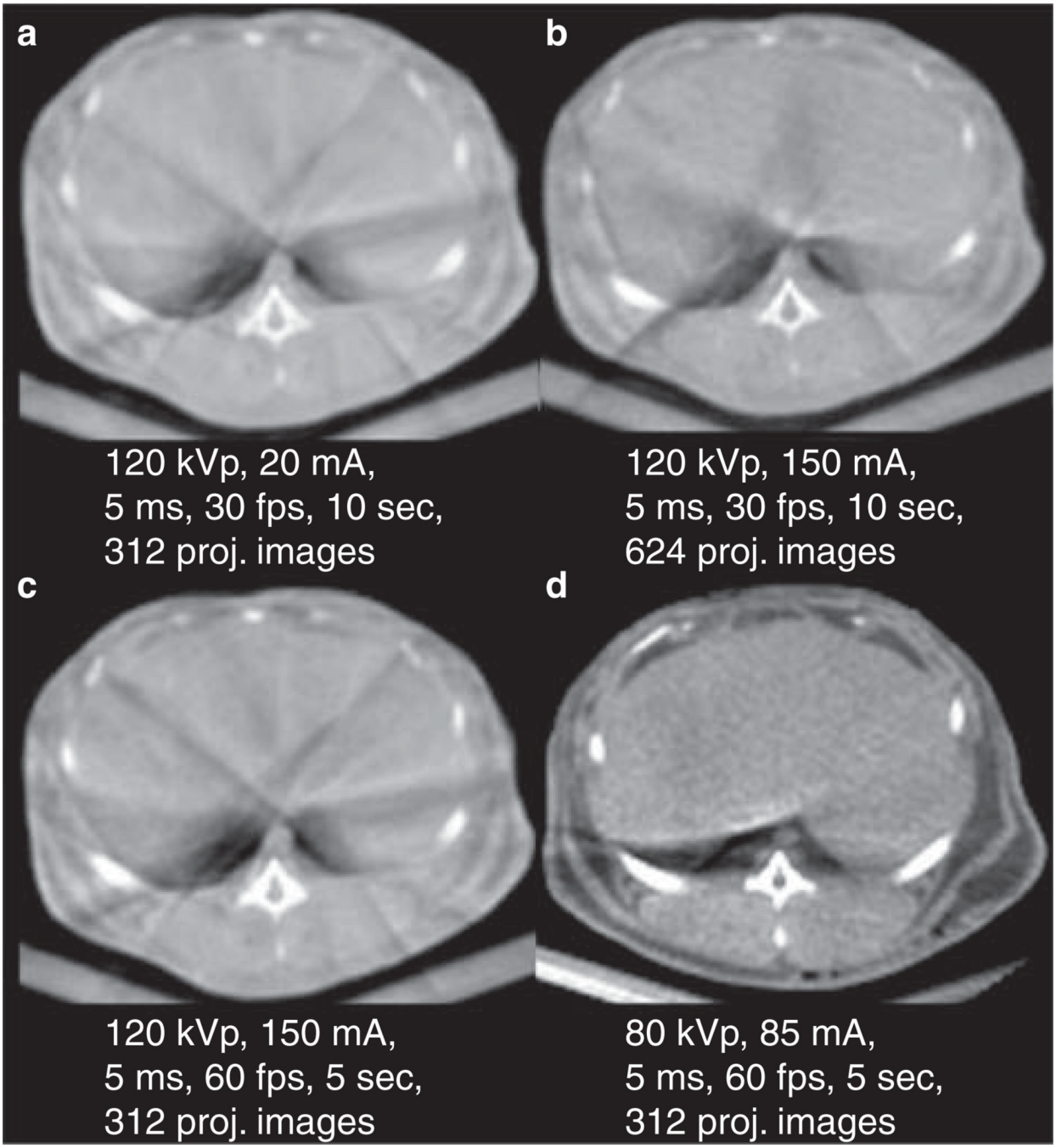

Figure 1.
Control rabbit imaged using various x-ray techniques (a–d correspond to protocol P1–P4 in Table I). Techniques a, b, and c are commercially available and technique d is a prototype. Of the commercially available protocols, protocol c had the best image quality according to the reviewers. And protocol d (prototype protocol) had the best overall IQ.

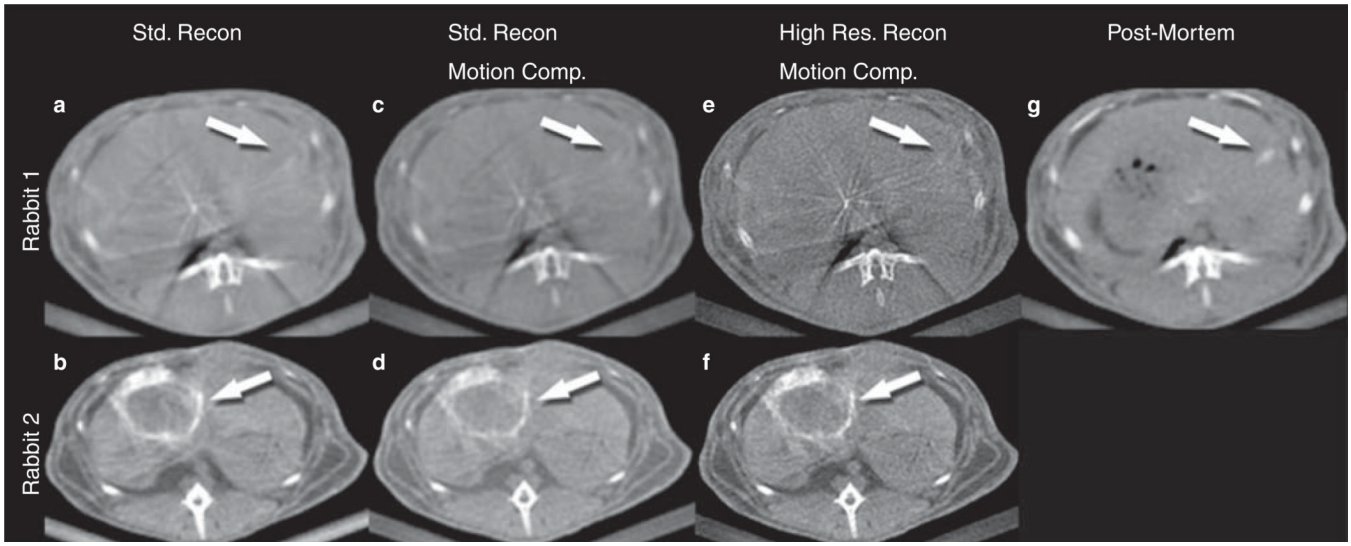

Figure 2.

Rabbit 1 (R1) images were acquired using the best commercially available x-ray technique (c in Figure 1, P3 in Table I), and rabbit 2 (R2) images were acquired using the prototype x-ray technique (d in Figure 1, P4 in Table I). A number of 3D reconstruction and motion compensation combinations were applied: Standard resolution reconstruction (a and b), motion compensation applied in addition to standard reconstruction (c and d), high resolution reconstruction with motion compensation (e and f). R1-g is a control image after euthanasia processed with standard reconstruction (to serve as a comparison image without motion). Tumor delineation improved with motion compensation and high resolution reconstruction (compare features indicated by arrows).

Table I

C-arm cone beam CT x-ray acquisition protocols. All protocols but the last (P4) are commercially available. The last two protocols (P3 and P4) resulted in the best image quality (kVp-kilo voltage potential, mA-milliamperes, ms-milliseconds, FPS-frames per second, mm-millimeter, and API-approximate number of projection images).

Protocol	Tube voltage kVp	Tube current mA	Frame length ms	Frames per second	Scan time sec	Detector Binning	Pixel Size mm^2	API
P1	120	200	5	30	10 sec	2×2	0.37	312
P2	120	150	5	60	10 sec	4×4	0.74	624
P3	120	150	5	60	5 sec	4×4	0.74	312
P4	80	85	5	60	5 sec	4×4	0.74	312

Minim Invasive Ther Allied Technol. Author manuscript; available in PMC 2013 December 11.